

以 5-甲基-3-吡唑甲酸为配体的钴(II)、镍(II)配合物的合成、晶体结构和性质

程美令^{*,1} 王 沈¹ 唐李志鹏¹ 刘 琦^{*,1,2}

(¹ 常州大学石油化工学院, 江苏省绿色催化材料和技术重点实验室, 常州 213164)

(² 南京大学配位化学国家重点实验室, 南京 210023)

摘要: 以 5-甲基-3-吡唑甲酸(H₂MPCA)为主配体, 桥联配体 4,4'-联吡啶(4,4'-bpy)和吡嗪(py₂)为辅助配体, 合成了 2 个新的配合物 {[Co(HMPCA)₂(4,4'-bpy)]₂·5H₂O}_n(**1**)和 [[Ni(HMPCA)₂(py₂)]·5H₂O]_n(**2**), 并用元素分析、红外光谱、X 射线单晶衍射结构分析、热重分析等对其进行了表征。配合物 **1** 属于正交晶系, 空间群为 *Pccn*, 配合物 **2** 属于单斜晶系, 空间群为 *P2/c*。在 **1** 和 **2** 中, 金属离子都位于一个扭曲的八面体配位环境中, 分别由 4,4'-联吡啶(**1**)和吡嗪(**2**)两端的氮原子桥联 2 个相邻的金属离子, 形成一维链状聚合物。考察了配合物 **1** 和 **2** 的热稳定性、荧光性能和磁性。

关键词: 钴; 镍; 5-甲基-3-吡唑甲酸; 晶体结构; 荧光; 磁性

图分类号: O614.81+2; O614.81+3

文献标识码: A

文章编号: 1001-4861(2016)08-1457-10

DOI: 10.11862/CJIC.2016.184

Syntheses, Crystal Structures and Properties of Cobalt(II) and Nickel(II) Complexes Based on 5-Methyl-1*H*-pyrazole-3-carboxylic Acid Ligand

CHENG Mei-Ling^{*,1} WANG Shen¹ TANG Li-Zhi-Peng¹ LIU Qi^{*,1,2}

(¹ School of Petrochemical Engineering and Jiangsu Key Laboratory of Advanced Catalytic Materials and Technology, Changzhou University, Changzhou, Jiangsu 213164, China)

(² State Key Laboratory of Coordination Chemistry, Nanjing University, Nanjing 210023, China)

Abstract: Two new 1D chain-typed coordination polymers, {[Co (HMPCA)₂ (4,4'-bpy)]₂ · 5H₂O}_n (**1**) and [[Ni(HMPCA)₂(py₂)]·5H₂O]_n(**2**) (H₂MPCA=5-methyl-1*H*-pyrazole-3-carboxylic acid, 4,4'-bpy=4,4'-bipyridine, py₂=pyrazine), have been synthesized and characterized by elemental analysis, IR spectra, single crystal X-ray diffraction and thermogravimetric analysis. Complex **1** crystallizes in the orthorhombic system, space group *Pccn*, and **2** crystallizes in the monoclinic system, space group *P2/c*. In **1** and **2**, metal ions are both located in an octahedral geometry, coordinated by two nitrogen atoms and two oxygen atoms from two HMPCA⁻ anions, and linked by two nitrogen atoms from 4,4'-bpy ligands (**1**) and py₂ ligands (**2**), respectively, forming a 1D chain-typed coordination polymer. The thermal stability, luminescent properties and magnetic properties of them have also been investigated. CCDC: 1445391, **1**; 1445392, **2**.

Keywords: cobalt(II); nickel(II); 5-methyl-1*H*-pyrazole-3-carboxylic acid; crystal structure; photoluminescence; magnetic properties

收稿日期: 2016-04-01。收修改稿日期: 2016-06-02。

国家自然科学基金(No.21101018, 20971060)、江苏省高校自然科学研究面上项目(No.13KJB150001)、南京大学配位化学国家重点实验室开放课题和江苏省先进催化与绿色制造协同创新中心创新型人才支持项目资助。

*通信联系人。E-mail: chengmeiling01@163.com; liuqi62@163.com; Tel: 0519-86330185; 会员登记号: S060018987P。

0 Introduction

In the past decades, the design and construction of the supramolecular complexes constructed by coordination bonds and/or other weak cooperative interactions have become a very attractive research field in coordination chemistry and materials chemistry^[1-4]. The interest comes from the outstanding topological structures and unique potential applications in many fields, such as gas storage^[5-8], heterogeneous catalysis^[9-10], sensors^[11], lithium-ion batteries^[12-14]. Synthesis of supramolecular complexes through self-assembly is a complicated process, highly influenced by a lot of factors, such as the nature of organic ligands, the coordination geometry of metal ions, metal-ligand ratio, pH value, solvent system, temperature, template agents and counter anions. There is no doubt that selection and reasonable use of characteristic ligands is the key point in the construction of complexes^[15-20]. Recently, N-heterocyclic carboxylic acids with good coordination capacities in multi-coordination modes by the N and O donor atoms on the N-heterocyclic rings and the carboxyl groups, are increasingly used in construction of complexes. The nitrogen atoms and carboxylic oxygen atoms can not only coordinate to metals, but also act as a donor and/or acceptor in hydrogen bond interactions for assembling the complex into high-dimensional supramolecular networks. For example, organic ligand 5-methyl-1*H*-pyrazole-3-carboxylic acid (H₂MPCA) has been widely used to synthesize various supramolecular architectures containing transition and main group metal ions, in which, H₂MPCA ligand has both bridging and chelating coordination modes to bind metal centers^[21-25]. On the other hand, the chelate N ancillary ligands, such as 2,2'-bipyridine (2,2'-bpy) and 1,10-phenanthroline (phen), were also utilized in the synthesis processes, which can adjust the coordination structures by occupying the terminal position^[23]. As we all known, bipyridine (4,4'-bpy)^[26] and pyrazine (pyz)^[25] are good candidates for molecular building blocks, due to their rod-like rigidity and length. But, the researches of using these bridging N

ancillary ligands to construct H₂MPCA containing complexes have been less explored, only two 1D coordination polymers, $\{[\text{Cu}_2(4,4'\text{-bpy})_2(2,2'\text{-bpy})(\text{MPCA})_2] \cdot 6\text{H}_2\text{O}\}_n$ ^[21] and $\{[\text{Co}(\text{HMPCA})_2(\text{pyz})] \cdot 5\text{H}_2\text{O}\}_n$ were reported^[25]. As the continuation of our research in constructing functional metal complexes containing N-heterocyclic carboxylic acids^[22-25,27-30], we carried out the reactions of H₂MPCA with corresponding metal salts and bridging N ancillary 4,4'-bpy and pyz, and isolated two new complexes, $\{[\text{Co}(\text{HMPCA})_2(4,4'\text{-bpy})]_2 \cdot 5\text{H}_2\text{O}\}_n$ (**1**) and $\{[\text{Ni}(\text{HMPCA})_2(\text{pyz})] \cdot 5\text{H}_2\text{O}\}_n$ (**2**). In this paper, the synthesis, crystal structures, photoluminescent and magnetic properties of the coordination polymers **1** and **2** were described.

1 Experimental

1.1 Materials and methods

All solvents and starting materials for synthesis were purchased commercially and were used as received. H₂MPCA was prepared following the literature method^[31]. The elemental analysis (C, H and N) was performed on a Perkin-Elmer 2400 Series II element analyzer. FTIR spectra were recorded on a Nicolet 460 spectrophotometer in the form of KBr pellets in the range of 4 000~400 cm⁻¹. Single-crystal X-ray diffraction measurements of **1** and **2** were carried out with a Bruker Smart Apex II CCD diffractometer at 296(2) K. Thermogravimetric analysis (TGA) experiments were carried out on a Dupont thermal analyzer from room temperature to 800 °C at a heating rate of 10 °C · min⁻¹ under N₂ atmosphere. Powder X-ray diffraction (PXRD) determinations were performed on an X-ray diffractometer (D/max 2500 PC, Rigaku) with Cu K α radiation (0.154 06 nm). The operating voltage and current were 60 kV and 300 mA, respectively. The luminescent spectra of the solid samples were recorded with a Cary Eclipse spectrometer. The magnetic susceptibility measurements for crystalline sample were measured over the temperature range of 1.8~300 K with a Quantum Design MPMS-XL7 SQUID magnetometer using an applied magnetic field of 2 000 Oe. Data were corrected for the diamagnetic contribution calculated from Pascal

constants.

1.2 Preparation of $[\{\text{Co}(\text{HMPCA})_2(4,4'\text{-bpy})\}_2 \cdot 5\text{H}_2\text{O}]_n$ (**1**)

To a solution containing H_2MPCA (0.025 2 g, 0.2 mmol) and $4,4'\text{-bpy} \cdot 2\text{H}_2\text{O}$ (0.076 8 g, 0.4 mmol) in DMF (2.0 mL) was added a solution of $\text{Co}(\text{OAc})_2 \cdot 4\text{H}_2\text{O}$ (0.024 9 g, 0.1 mmol) in MeOH (4.0 mL). The resulting solution was stirred for 30 min, followed by being placed into 15 mL Teflon-lined autoclave under autogenous pressure and heated at 120 °C for 24 h, then the solution was cooled to the ambient temperature at the rate of 5 °C \cdot h⁻¹. After filtration, the product was washed with deionized water and then dried, and red crystals of **1** (0.026 5 g, 52%, based on H_2MPCA) suitable for X-ray diffraction analysis were obtained. Anal. Calcd. for $\text{C}_{40}\text{H}_{44}\text{Co}_2\text{N}_{12}\text{O}_{13}$ (%): C, 47.16; H, 4.35; N, 16.50; Found (%): C, 46.01; H, 4.82; N, 16.07. IR spectrum (cm^{-1} , KBr pellet): 3 431 (s), 3 182 (m), 3 132 (m), 3 084 (m), 2920 (m), 2 854 (m), 1 681 (s), 1 605 (vs), 1 535 (m), 1 495 (m), 1 420 (s), 1 383 (m), 1 343 (s), 1 293 (s), 1 217 (w), 1 191 (w), 1 089 (w), 1 067 (w), 1 027 (m), 1 013 (m), 818 (m), 796 (m), 688 (w), 634 (m), 576 (w), 528 (w), 455 (w).

1.3 Preparation of $[\{\text{Ni}(\text{HMPCA})_2(\text{pyz})\} \cdot 5\text{H}_2\text{O}]_n$ (**2**)

To a solution containing H_2MPCA (0.025 2 g, 0.2 mmol) and pyz (0.016 0 g, 0.2 mmol) in deionized water (5.0 mL) was added a solution of $\text{Ni}(\text{OAc})_2 \cdot 4\text{H}_2\text{O}$ (0.049 9 g, 0.2 mmol) in deionized water (5.0 mL). The resulting solution was stirred for 30 min, followed by being placed into 25 mL Teflon-lined autoclave under autogenous pressure and heated at 180 °C for 24 h, then is was cooled to the ambient temperature at the rate of 5 °C \cdot h⁻¹. After filtration, the product was washed with deionized water and then dried, and blue crystals of **2** (0.028 7g, 60%, based on H_2MPCA) suitable for X-ray diffraction analysis were obtained. Anal. Calcd. for $\text{C}_{14}\text{H}_{24}\text{NiN}_6\text{O}_9$ (%): C, 35.10; H, 5.05; N, 17.54; Found

(%): C, 35.01; H, 5.31; N, 17.23. IR spectrum (cm^{-1} , KBr pellet): 3 379 (m), 3 200 (m), 3 140 (m), 3 110 (m), 2 969 (w), 2 850 (w), 1 610 (vs), 1 493 (w), 1 418 (s), 1 324 (m), 1 281 (s), 1 212 (m), 1 118 (w), 1 160 (w), 1 050 (m), 1 025 (m), 843 (w), 794 (m), 688 (w), 563 (w), 483 (m), 446 (w).

1.4 X-ray crystallography

Single-crystal X-ray diffraction measurements of **1** and **2** were carried out with a Bruker Smart Apex II CCD diffractometer at 296(2) K (**1**) and 293(2) K (**2**). Intensities of reflections were measured using graphite-monochromatized Mo $K\alpha$ radiation ($\lambda = 0.071\ 073\ \text{nm}$) with the φ - ω scans mode in the range of 2.809° ~28.071° (**1**) and 2.433° ~27.631° (**2**). The structure was solved by direct methods using the SHELXS program of the SHELXTL package and refined with SHELXL^[32]. For **1**, the lattice water molecule (O4) was fixed with constrained parameters and refined with an occupancy factor of 0.25. In the case of **2**, two free water molecules bearing O3 and O4 atoms were found to be disordered over two positions with an occupancy ratio of 0.5/0.5 for O(3)/O(3A) and O(4)/O(4A). Another lattice water molecule (O5) was fixed with constrained parameters and refined with an occupancy factor of 0.5. Anisotropic thermal factors were assigned to all the non-hydrogen atoms. Hydrogen atoms on O4 atom in **1** were not located. All other hydrogen atoms attached to C were placed geometrically and allowed to ride during subsequent refinement with an isotropic displacement parameter fixed at 1.2 times U_{eq} of the parent atoms. H atoms bonded to O or N atoms were first located in difference Fourier maps and then placed in the calculated sites and included in the refinement. Crystallographic data parameters for structural analyses are summarized in Table 1.

CCDC: 1445391, **1**; 1445392, **2**.

Table 1 Crystal structure parameters of the compounds **1** and **2**

Compound	1	2
Empirical formula	$\text{C}_{40}\text{H}_{44}\text{Co}_2\text{N}_{12}\text{O}_{13}$	$\text{C}_{14}\text{H}_{24}\text{NiN}_6\text{O}_9$
Formula weight	1 018.73	479.10
Crystal size / mm	0.26×0.24×0.24	0.26×0.24×0.20

Continued Table 1

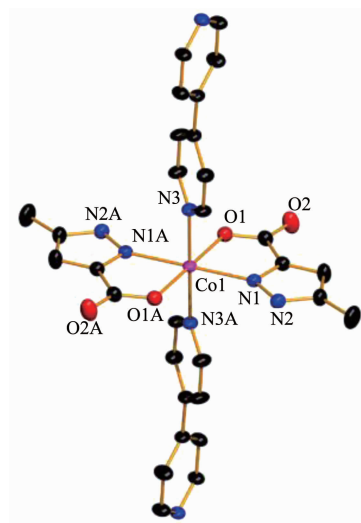
Crystal system	Orthorhombic	Monoclinic
Space group	<i>Pccn</i>	<i>P2/c</i>
<i>a</i> / nm	2.082 3(3)	0.858 0(3)
<i>b</i> / nm	0.918 7(12)	0.709 2(2)
<i>c</i> / nm	1.434 06(17)	1.724 9(6)
β / (°)		103.882(6)
<i>V</i> / nm ³	2.743 4(6)	1.018 9(6)
<i>Z</i>	2	2
<i>D_c</i> / (g·cm ⁻³)	1.233	1.562
<i>F</i> (000)	1 052	500
μ (Mo <i>K</i> α) / mm ⁻¹	0.668	1.012
Index ranges (<i>h</i> , <i>k</i> , <i>l</i>)	-27~24, -11~9, -17~18	-10~11, -9~8, -22~20
Total reflections	17 073	6 208
Independent reflections (<i>R_{int}</i>)	3 280 (0.059 1)	2 326 (0.031 8)
Refinement method	Full-matrix least-squares on <i>F</i> ²	
Data, restraints, parameters	3 280, 2, 157	2 326, 10, 161
Goodness-of-fit on <i>F</i> ²	1.032	1.028
<i>R</i> ₁ , <i>wR</i> ₂ [<i>I</i> > 2 σ (<i>I</i>)]	0.067 5, 0.216 7	0.039 4, 0.101 2
<i>R</i> ₁ , <i>wR</i> ₂ (all data)	0.111 1, 0.251 4	0.050 5, 0.107 2
Largest diff. peak and hole / (e·nm ⁻³)	1 157 and -371	498 and -544

2 Results and discussion

2.1 IR spectrum

The IR spectra of complexes **1** and **2** reflect the binding patterns of H₂MPCA, 4,4'-bpy and pyz (Fig.S1 in supplementary materials). The strong and broad

absorption band around 3 200~3 600 cm⁻¹ region is assigned as characteristic peak of OH vibration, indicating that water molecules exist in the complexes. The absorption peak between 1 690 cm⁻¹ and 1 730 cm⁻¹ is not observed, showing all carboxylic groups are deprotonated. The strong peaks at 1 605 cm⁻¹ (**1**), 1 610



Hydrogen atoms and solvent molecules were omitted for clarity; Symmetry codes: A: 1-*x*, 1-*y*, 2-*z*

Fig.1 Coordination environment of Co(II) ion in **1** with thermal ellipsoid at 30% probability level

cm^{-1} (**2**), and $1\,420\text{ cm}^{-1}$ (**1**), $1\,418\text{ cm}^{-1}$ (**2**) are the $\nu_{\text{as}}(\text{COO}^-)$ and $\nu_{\text{s}}(\text{COO}^-)$ stretching mode of the coordinated HMPCA⁻ ligand, respectively^[33-35]. For complex **1**, the weak absorption at $3\,000\text{ cm}^{-1}$ is the $\nu_{\text{as}}(\text{C-H})$ bent vibration of 4,4'-bpy. For complex **2**, the absorbances between $1\,050$ and $1\,212\text{ cm}^{-1}$ are assignable to pyz bands^[36].

2.2 Crystal structures of **1** and **2**

X-ray crystal structure analysis reveals that **1** crystallizes in the orthorhombic system space group *Pccn*. The asymmetric unit of **1** contains a half of Co (II) ion, one HMPCA⁻ anion, half of a 4,4'-bpy, one and a half lattice water molecules. The coordination sphere of Co(II) is defined by two carboxylate oxygen atoms, two nitrogen atoms from two HMPCA⁻ anions, and two nitrogen atoms from two 4,4'-bpy ligands, leading to a hexa-coordinated octahedral geometry. The equatorial position are occupied by O1, O1A, N1, and N1A atoms, proved by that the sum of the bond angles of O1A-Co1-N1A ($78.48(11)^\circ$), N1-Co1-O1 ($78.48(11)^\circ$), N1-Co1-O1A ($101.52(11)^\circ$) and O1-Co1-N1A ($101.52(11)^\circ$) is equal to 360° , and N3 and N3A atoms are located in the axial positions (Fig.1 and Table 2). As a bidentate ligand, the HMPCA⁻ anion chelates one Co(II) atom with pyrazole N atom and

carboxyl O atom to form a five membered ring. As shown in Fig.2, two crystallographically equivalent ions, Co1 and Co1A are linked by two N atoms (N3 and N3A) from 4,4'-bpy in a bridging fashion, generating an infinite 1D chain. The length of Co-O1 bond is $0.207\,6(3)\text{ nm}$, and the Co-N bonds are in the range of $0.214\,4(3)\sim 0.216\,5(3)\text{ nm}$, which are close to those Co-O (Co1-O1 $0.211\,6(5)\text{ nm}$), Co-N (Co1-N1 $0.208\,2(5)\text{ nm}$) in the reported Co(II) complex $[\text{CoCl}_4(\text{Athpp})_2]\cdot 2\text{H}_2\text{O}$ (Athpp=3-amino-1,4,5,6-tetrahydropyrrrolo[3,4-*c*]pyrazole)^[37]. The average bond length of Co-N is longer than that of Co-O, showing that the strength of cobalt ion coordinated with nitrogen atoms are weaker than that of oxygen atoms from HMPCA⁻ ligands in **1**. By the function of the hydrogen bond O3-H3X \cdots O2C (Symmetry codes: C: $x, 1+y, -1+z$) and O3-H3Y \cdots O1D (Symmetry codes: D: $1-x, 1/2+y, 3/2-z$), the solvent water molecules are embedded in the chain. Finally, these 1D chains are extended into 3D structure by the N2-H2 \cdots O2B (Symmetry codes: B: $x, 1/2-y, -1/2+z$) hydrogen-bonding interactions (Fig.3).

2 crystallizes in the monoclinic system space group *P2/c*. The asymmetric unit of **2** contains half of one Ni(II) ion, one HMPCA⁻ anion, half of one pyz,

Table 2 Selected bond lengths (nm) and angles ($^\circ$) for the compounds **1** and **2**

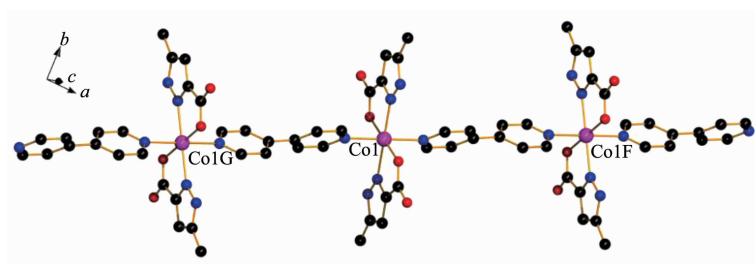
Compound 1					
Co1-O1	0.207 6(3)	Co1-O1A	0.207 6(3)	Co1-N1	0.214 4(3)
Co1-N1A	0.214 4(3)	Co1-N3	0.216 5(3)	Co1-N3A	0.216 5(3)
O1-Co1-O1A	180.0	O1A-Co1-N1A	78.48(11)	O1-Co1-N1A	101.52(11)
O1A-Co1-N1	101.52(11)	O1-Co1-N1	78.48(11)	N1-Co1-N1A	180.00(8)
O1A-Co1-N3	89.51(12)	O1-Co1-N3	90.49(12)	N1A-Co1-N3	89.23(12)
N1-Co1-N3	90.77(12)	O1A-Co1-N3A	90.49(12)	O1-Co1-N3A	89.51(12)
N1A-Co1-N3A	90.77(12)	N1-Co1-N3A	89.23(12)	N3-Co1-N3A	180.00(6)
Compound 2					
Ni1-N1	0.206 19(19)	Ni1-N1A	0.206 19(19)	Ni1-O1	0.207 04(18)
Ni1-O1A	0.207 04(18)	Ni1-N4	0.213 6(3)	Ni1-N3	0.216 6(3)
N1-Ni1-N1A	178.99(11)	N1-Ni1-O1	79.85(7)	N1A-Ni1-O1	100.15(7)
N1-Ni1-O1A	100.15(7)	N1A-Ni1-O1A	79.85(7)	O1-Ni1-O1A	179.67(9)
N1-Ni1-N4	90.50(5)	N1A-Ni1-N4	90.50(5)	O1-Ni1-N4	90.16(4)
O1A-Ni1-N4	90.16(4)	N1-Ni1-N3	89.50(5)	N1A-Ni1-N3	89.50(5)
O1-Ni1-N3	89.84(4)	O1A-Ni1-N3	89.84(4)	N4-Ni1-N3	180.0

Symmetry codes: A: $1-x, 1-y, 2-z$ for **1**; A: $2-x, y, 1/2-z$ for **2**

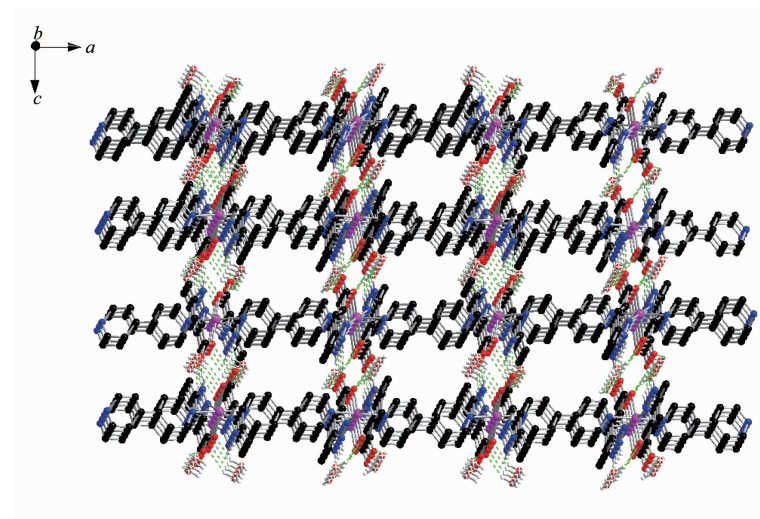
Table 3 Hydrogen bond parameters ($^{\circ}$) for the compound **1**

D-H \cdots A	$d(\text{D-H}) / \text{nm}$	$d(\text{H}\cdots\text{A}) / \text{nm}$	$d(\text{D}\cdots\text{A}) / \text{nm}$	$\angle \text{D-H}\cdots\text{A} / (^{\circ})$
N2-H2 \cdots O2B	0.083	0.196	0.278 5(4)	169
O3-H3X \cdots O2C	0.084	0.216	0.278 7(6)	132
O3-H3Y \cdots O1D	0.085	0.210	0.289 1(5)	154
C6-H6 \cdots O3E	0.093	0.257	0.326 0(6)	132
C10-H10 \cdots O3H	0.093	0.253	0.312 8(6)	122

Symmetry codes: B: $x, 1/2-y, -1/2+z$; C: $x, 1+y, -1+z$; D: $1-x, 1/2+y, 3/2-z$; E: $1-x, -1/2+y, 3/2-z$; H: $1-x, 1-y, 1-z$



Hydrogen atoms were omitted for clarity; Symmetry codes: F: $3/2-x, 3/2-y, z$; G: $1/2-x, 1/2-y, z$

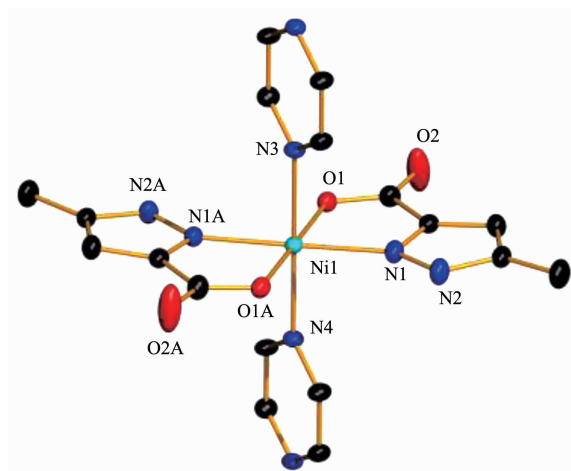
Fig.2 One-dimension chain of **1**

Only hydrogen atoms involved in the hydrogen bonds are shown; Hydrogen bonds are indicated by dashed lines, the lattice water molecules are shown in the front ellipses mode

Fig.3 Three-dimension structure of **1**

two and half free water molecules. As illustrated in Fig.4, Ni(II) ion is located in a distorted octahedral geometry, coordinating with two N atoms (N1, N1A), two O atoms (O1, O1A) from two chelating HMPCA $^{-}$ anions, and two N atoms (N3, N4) from two pyz ligands. The equatorial position are occupied by O1, O1A, N1, and N1A atoms, proved by that the sum of the bond angles of O1A-Ni1-N1A($79.85(7)^{\circ}$), N1-Ni1-

O1($79.85(7)^{\circ}$), N1-Ni1-O1A($100.15(7)^{\circ}$) and O1-Ni1-N1A($100.15(7)^{\circ}$) is equal to 360° , and N3 and N4 atoms are located in the axial positions (Table 2). The length of Ni-O bond are 0.207 04(18) nm, and the Ni-N bonds are in the range of 0.206 19(19)~0.216 6(3) nm, which are close to those Ni-O (Ni1-O1 0.209 80(13) nm), Ni-N (Ni1-N1 0.206 82(14) nm) in the reported Ni(II) complex $[\text{Ni}(\text{HMPCA})_2(\text{ImH})_2] \cdot 2\text{H}_2\text{O}$ [24]. The

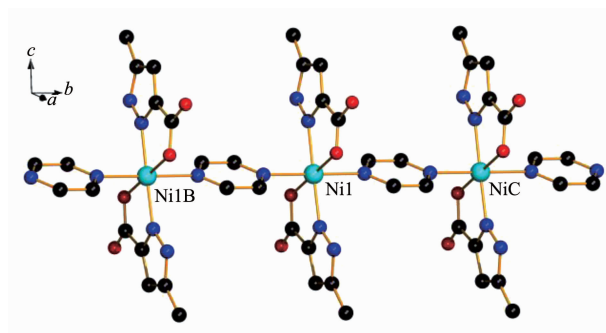


Hydrogen atoms and solvent molecules were omitted for clarity; Symmetry codes: A: $2-x, y, 1/2-z$

Fig.4 Coordination environment of Ni(II) ion in **2** with thermal ellipsoid at 30% probability level

average bond length of Ni-N is longer than that of Ni-O, showing that the strength of Ni(II) ion coordinated with nitrogen atoms are weaker than that of oxygen atoms from HMPCA⁻ ligands in **2**. Adjacent Ni(II) centers are linked by one pyz ligand in a bridging

mode to form an infinite 1D chain (Fig.5), in which the Ni1...Ni1B separation is 0.709 2 (2) nm. Five halves of solvent water molecules (O3, O3A, O4, O4A and O5) are not discussed about the hydrogen bond interactions.



Hydrogen atoms and solvent molecules were omitted for clarity; Symmetry codes: B: $x, -1+y, z$; C: $x, 1+y, z$

Fig.5 One-dimension chain government of the coordination compound **2**

2.3 Thermogravimetric analysis

So as to examine the thermal stability of the compounds **1** and **2**, the thermogravimetric analysis were carried out from ambient temperature up to 800 °C (Fig.S2). For **1**, the first weight loss of 8.89% between 50 and 206 °C is attributed to the loss of lattice water molecules (Calcd. 8.84%). The second degradation stage is in the range of 206~230 °C with weight loss of 30.76%, corresponding to the loss of 4,4'-bpy molecules (Calcd. 30.66%). The third

degradation stage is in the range of 230~460 °C, corresponding to the loss of HMPCA⁻ ligands, and the remaining material finally degrades to CoO (Calcd. 14.71%, Found 14.96%). For **2**, the first weight loss of 8.02% between 110 and 224 °C is attributed to the loss of two lattice water molecules (Calcd. 7.52%). The second degradation stage is in the range of 224~356 °C with weight loss of 26.20%, corresponding to the loss of three lattice water molecules and one pyz molecule (Calcd. 27.99%). Above 356 °C, the

remaining material decomposes gradually.

2.4 Powder X-ray diffraction

The PXRD patterns of title complexes are measured at room temperature for checking the phase purity of the complexes (Fig.S3). The operating voltage and current were 60 kV and 300 mA, respectively. Peaks of the experimental and simulated PXRD patterns are in accordance with each other, indicating the superior phase purity of the complexes. The dissimilarities in intensity may be on account of the preferred orientation of the crystalline powder samples.

2.5 Fluorescence properties

The solid-state fluorescence of two complexes and free H₂MPCA were investigated at room temperature (Fig.S4). The strongest emission peaks for **1** and **2**, and free ligand all appear at ca. 425 nm ($\lambda_{\text{ex}}=376$ nm). According to the position and band shape, the emission bands for **1** and **2** are very similar to that of the free ligand, indicating that the emission bands of complexes **1** and **2** may be attributable to the internal charge transfer ($\pi \rightarrow \pi^*/n \rightarrow \pi^*$ transitions) of the ligand.

2.6 Magnetic properties

With an applied magnetic field of 2 000 Oe, the variable-temperature (1.8~300 K) magnetic susceptibility data were collected for a crystal sample of complexes **1** and **2** (Fig.6, 7). For complex **1**, the experimental $\chi_{\text{M}}T$ value is 2.497 emu·K·mol⁻¹, which is much larger than the spin-only value of 1.875 emu·K·mol⁻¹ for an uncoupled high-spin cobalt (II) ion (with $S=3/2$), indicating that an important orbital contribution is

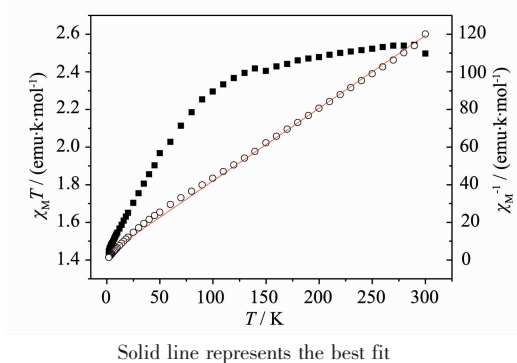


Fig.6 Temperature dependence of $\chi_{\text{M}}T$ (■) and χ_{M}^{-1} (○) for (**1**)

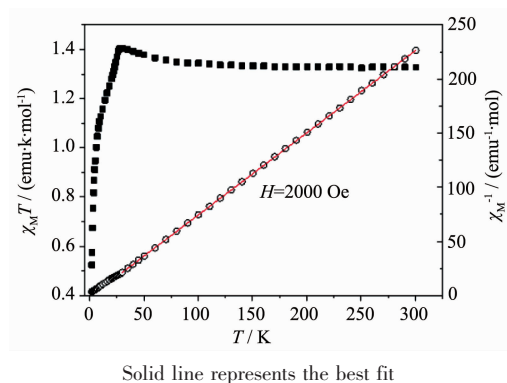


Fig.7 Temperature dependence of $\chi_{\text{M}}T$ (■) and χ_{M}^{-1} (○) for (**2**)

involved. The $\chi_{\text{M}}T$ value is different from the value of 2.972 emu·K·mol⁻¹ for the complex $[\text{Co}(\text{HMPCA})_2(\text{pyz})] \cdot 5\text{H}_2\text{O}$ [25] and that of 2.985 emu·K·mol⁻¹ for the complex $[\text{Co}(\text{pyz})(\text{H}_2\text{O})_4](\text{NO}_3)_2 \cdot 2\text{H}_2\text{O}$ [36], also different from the value of 2.1 emu·K·mol⁻¹ for $[\text{Co}(\text{acac})_2(\text{pyz})]$ [38]. As shown in Fig.6, when the temperature is lowered, the $\chi_{\text{M}}T$ value decreases continuously to 1.443 emu·K·mol⁻¹ at 1.8 K. Such behavior suggests the existence of antiferromagnetic interaction behavior even if the single-ion effects, such as spin-orbit coupling, distortion from regular stereochemistry, electron delocalization, and crystal field mixing of excited states into the ground state, may also be present [39]. The Curie-Weiss law ($\chi_{\text{M}}=C/(T-\theta)$) was used to fit the magnetic susceptibilities between 300 and 1.8 K. According to the fitting result, Curie constant of $C=2.59$ emu·K·mol⁻¹ and Weiss constant of $\theta=-8.67$ K can be obtained, indicating further that a antiferromagnetic coupling between Co(II) ions. For complex **2**, the experimental $\chi_{\text{M}}T$ value at 300 K is 1.327 emu·K·mol⁻¹, which is higher than that expected for spin-only value of Ni(II) ion (1.0 emu·K·mol⁻¹ with $g=2.0$) (Fig.7). As the temperature lowers to 1.8 K, the $\chi_{\text{M}}T$ value increases slowly to a maximum of about 1.405 emu·K·mol⁻¹ at 30 K, then decreases rapidly to a value of 0.524 emu·K·mol⁻¹ at 1.8 K. This behavior suggests that ferromagnetic interactions are operating in **2** in the high-temperature region of 30~300 K, which origins from magnetic exchange interactions Ni(II) ions between pyz ligand within the 1D chain. Similar

ferromagnetic interactions also exist in reported nickel complexes $[\text{Ni}(\text{SCN})_2(\text{pyrazine})_2]_n$ and $[\text{Ni}(\text{SCN})_2(\text{pyrazine})_2]$ [40]. The sharp decrease of $\chi_M T$ value at lower temperatures may be a consequence of interchains antiferromagnetic interactions in the 3D lattice, which favor a long-range antiferromagnetic ordering. The magnetic susceptibilities above 30 K follow the Curie-Weiss law $\chi_M = C/(T - \theta)$ with Curie constant of $1.32 \text{ emu} \cdot \text{K} \cdot \text{mol}^{-1}$ and Weiss constant of 1.935 K. The positive θ value also reveal the presence of ferromagnetic interaction in **2** in the high-temperature region. The magnetic susceptibilities of 30 ~2 K follow the Curie-Weiss law with Curie constant of $1.548 \text{ emu} \cdot \text{K} \cdot \text{mol}^{-1}$ and Weiss constant of -3.482 K. The negative θ value also reveal the presence of antiferromagnetic interaction in **2** in the low-temperature region.

3 Conclusions

In summary, we have successfully synthesized two new complexes with infinite 1D chains, $\{[\text{Co}(\text{HMPCA})_2(4,4'\text{-bpy})]_2 \cdot 5\text{H}_2\text{O}\}_n$ (**1**) and $\{[\text{Ni}(\text{HMPCA})_2(\text{pyz})] \cdot 5\text{H}_2\text{O}\}_n$ (**2**) by the reaction of H_2MPCA and N ancillary ligands with $\text{M}(\text{OAc})_2 \cdot 4\text{H}_2\text{O}$ ($\text{M} = \text{Co}, \text{Ni}$) respectively. The emission bands of complexes **1** and **2** may be attributable to the intraligand $\pi \rightarrow \pi^*/n \rightarrow \pi^*$ transitions. Magnetic properties of the complexes show that **1** exists the interaction of anti-ferromagnetism between two adjacent metal ions and **2** exists ferromagnetic interaction in the high-temperature region and antiferromagnetic interaction in the low-temperature region.

Supporting information is available at <http://www.wjhxxb.cn>

References:

- [1] Cook T R, Zheng Y R, Stang P J. *Chem. Rev.*, **2013**, **113**(1): 734-777
- [2] Hu X Y, Xiao T X, Lin C, et al. *Acc. Chem. Res.*, **2014**, **47**(7):2041-2051
- [3] Liu Q, Liu X X, Shi C D, et al. *Dalton Trans.*, **2015**, **44**: 19175-19184
- [4] Liu X X, Shi C D, Zhai C W, et al. *ACS Appl. Mater. Interfaces*, **2016**, **8**(7):4585-4591
- [5] Santra A, Senkovska I, Kaskel S, et al. *Inorg. Chem.*, **2013**, **52**(13):7358-7366
- [6] Gipson T J, Beobide G, Castillo O, et al. *Cryst. Growth Des.*, **2014**, **14**(8):4019-4029
- [7] Hu S, He K H, Zeng M H, et al. *Inorg. Chem.*, **2008**, **47**(12): 5218-5224
- [8] Chatterjee B, Noveron C J, Resendiz E J M, et al. *J. Am. Chem. Soc.*, **2004**, **126**(34):10645-10656
- [9] Brown J C, Miller M G, Johnson W M, et al. *J. Am. Chem. Soc.*, **2011**, **133**(31):11964-11966
- [10] Hagen M C, Ludovic V P, Gábor L, et al. *Organometallics*, **2005**, **24**(8):1819-1831
- [11] Gong Y N, Huang Y L, Jiang L, et al. *Inorg. Chem.*, **2014**, **53**(18):9457-9459
- [12] Ke F S, Wu Y S, Deng H. *J. Solid State Chem.*, **2015**, **223**: 109-121
- [13] Nagarathinam M, Saravanan K, Phua E J U, et al. *Angew. Chem.*, **2012**, **124**(24):5968-5972
- [14] Liu Q, Yu L L, Jiang L, et al. *Inorg. Chem.*, **2013**, **52**(6): 2817-2822
- [15] Hong M C, Zhao Y J, Su W P, et al. *Angew. Chem. Int. Ed.*, **2000**, **39**(14):2468-2470
- [16] Abrahams B F, Batten S R, Granna M J, et al. *Angew. Chem. Int. Ed.*, **1999**, **38**(10):1475-1477
- [17] Noro S, Kitaura R, Kondo M, et al. *J. Am. Chem. Soc.*, **2002**, **124**(11):2568
- [18] Dong Y B, Jiang Y Y, Li J, et al. *J. Am. Chem. Soc.*, **2007**, **129**(15):4520-4521
- [19] Wu S T, Long L S, Huang R B, et al. *Cryst. Growth Des.*, **2007**, **7**(9):1746-1752
- [20] Burrows A D, Cassar K, Friend R M W, et al. *CrystEngComm*, **2005**, **7**(89):548-550
- [21] Hu F L, Yin X H, Mi Y, et al. *Inorg. Chem. Commun.*, **2009**, **12**(7):628-631
- [22] Cheng M L, Han W, Liu Q, et al. *J. Coord. Chem.*, **2014**, **67**(2):215-226
- [23] TANG Li-Zhi-Peng(唐李志鹏), YANG Ming-Wei(杨明伟), CHENG Mei-Ling(程美令), et al. *Chinese J. Inorg. Chem. (无机化学学报)*, **2015**, **31**(3):603-610
- [24] HAN Wei(韩伟), CHENG Mei-Ling(程美令), LIU Qi(刘琦), et al. *Chinese J. Inorg. Chem. (无机化学学报)*, **2012**, **29**(9): 1997-2004
- [25] REN Yan-Qiu(任艳秋), HAN Wei(韩伟), CHENG Mei-Ling(程美令), et al. *Chinese J. Inorg. Chem. (无机化学学报)*, **2014**, **30**(11):2635-2644
- [26] Du M, Zhang Z H, Guo W, et al. *Cryst. Growth Des.*, **2009**, **9**

- (4):1655-1657
- [27]Chen L T, Tao F, Wang L D, et al. *Z. Anorg. Allg. Chem.*, **2013**,**639**(3/4):552-557
- [28]Su S, Cheng M L, Ren Y Q, et al. *Transition Met. Chem.*, **2014**,**39**(5):559-566
- [29]Xia Q H, Ren Y Q, Cheng M L, et al. *J. Coord. Chem.*, **2015**,**68**(10):1688-1704
- [30]Wang L D, Tao F, Cheng M L, et al. *J. Coord. Chem.*, **2012**,**65**(6):923-933
- [31]Crane J D, Fox O D, Sinn E. *J. Chem. Soc., Dalton Trans.*, **1999**(9):1461-1465
- [32]Sheldrick G M. *SHELXS-97, Program for X-ray Crystal Structure Determination*, University of Göttingen, Germany, **1997**.
- [33]Zhu E J, Liu Q, Chen Q, et al. *J. Coord. Chem.*, **2009**,**62**(15):2449-2456
- [34]Liu Q, Li Y Z, Song Y, et al. *J. Solid State Chem.*, **2004**,**177**(12):4701-4705
- [35]Nakamoto K. *Infrared and Raman Spectra of Inorganic and Coordination Compounds*. 4th Ed. New York: Wiley, **1986**.
- [36]Holman K T, Hassan H H, Samih I, et al. *Polyhedron*, **2005**,**24**(2):221-228
- [37]CHU Zhao-Jing(储兆晶), BAI Xiao-Guang(白晓光), WANG Yu-Cheng(王玉成), et al. *Chinese J. Inorg. Chem.* (无机化学学报), **2014**,**30**(4):945-951
- [38]Ma B Q, Gao S, Yi T, et al. *Polyhedron*, **2001**,**20**(11):1255-1261
- [39]Kahn O. *Molecular Magnetism*. Weinheim: VCH, **1993**.
- [40]Wriedt M, Jeß I, Näther C. *Eur. J. Inorg. Chem.* **2009**:1406-1413